

The Effects of Blockage on the Performance of Small Propellers

D. Verstraete¹ and R. MacNeill¹

¹School of Aerospace, Mechanical and Mechatronic Engineering,
The University of Sydney, Sydney, New South Wales, 2006, Australia

Abstract

When operating in the proximity of a fuselage, the performance of a propeller can be significantly affected. The blockage ratio, the ratio between the propeller diameter and the diameter of the fuselage, directly impacts the efficiency of the propeller and causes a shift in the advance ratio at which peak efficiency occurs. Whereas well characterized for larger general aviation propellers, the effects of propeller blockage for small propellers used on unmanned aircraft remain largely uninvestigated. The current article presents initial results of wind tunnel tests of small propellers with and without a fuselage installed. It is shown that the blockage effect can be more pronounced for small propellers than for larger propellers.

Introduction

As a result of rapid innovation, unmanned aircraft systems (UAS), or drones, are now commercially available on a large scale. UAS are in use for a large variety of missions, including in emergency assistance and disaster response, to monitor wildlife, to protect sensitive ecosystems, and to manage and monitor the environment [1]. The majority of UAS, especially at the smaller scale, are propeller-driven [2]. The efficiency of the powertrain and propeller is crucial for the performance of the vehicle, and a great deal of research is thus focused on more efficient powertrain technologies for small UAS [2–7]. However, small UAS currently primarily employ commercial off-the-shelf propellers which offer a low-cost, readily available solution [7]. Public performance data is limited for these propellers since manufacturers do not generally publish complete sets of data. This issue has been addressed over the last decade with independent testing and publishing of performance data [8–10]. To date research has not included the effects of installation on propeller performance even though these effects may prove crucial in optimal propeller selection.

The fuselage blockage effect is the result of a mutual interference between a propeller and fuselage. Fuselage blockage is comprised of two separate effects which arise from the aerodynamic interaction between a propeller and fuselage in close proximity. The ‘body interference effect’ results from the perturbed airflow through the propeller due to the influence of the fuselage. The ‘scrubbing effect’ reduces effective thrust due to an increase in drag when the fuselage is positioned within the propeller slipstream.

The body interference effect is a change in propeller efficiency caused by the proximity of the fuselage. In the regions closest to the rotation axis, the axial velocity of the air is significantly reduced. As a result, airfoil sections experience an increased angle of attack, which leads to an increase in thrust but also an increase in required power. Depending on the operating conditions, the increase in thrust may lead to an ‘apparent’ increase in propulsive efficiency. This occurs because the local flow velocity is slower than the freestream, so the true advance ratio is lower than the apparent advance ratio, based in the freestream. Since the propeller is operating in a region of reduced velocity, less mass flows through the propeller disk which results in

a reduction in net efficiency [11]. If adjusted for the true local velocity, the efficiency decreases as expected, however this velocity is not easy to measure. Due to reduced-velocity flow at the propeller disk, the efficiency also peaks at a different ‘apparent’ advance ratio when body interference is in effect [12].

The scrubbing effect, also known as slipstream effect, is the reduction in effective thrust due to an increase in drag of a fuselage within the propeller slipstream. In a puller configuration, the large velocity of a propeller slipstream increases the dynamic pressure around the fuselage. Furthermore, there is an increase in turbulence and the addition of a rotational component to the airflow in the direction of propeller rotation. As a result, the body drag of the fuselage increases [13]. The increase in drag of the body reduces the overall propulsive efficiency of the system. This effect is less pronounced with a pusher configuration, as the fuselage is located in the slower propeller inflow region.

The blockage effect depends on the blockage ratio, B , which is defined as:

$$B = \frac{D_{fus}}{D}, \quad (1)$$

where D_{fus} is the fuselage maximum diameter, and D is the propeller diameter. For general aviation propellers, it is suggested that fuselage blockage is negligible when the blockage ratio is below a critical value. Estimates of the critical blockage ratio range between 0.33 and 0.42 [14–17]. Efficiency reduces by 1% for every 10% increase in the blockage ratio beyond the critical value [15] with a typical decrease of around 5% due to the scrubbing effect for light general aviation aircraft with a puller configuration [18]. For small UAS this effect is expected to be more pronounced as both the propeller and fuselage are operated at significantly lower Reynolds numbers.

This article addresses installation effects for small propellers and UAS by investigating the mutual interference between fuselage and propeller, known as fuselage blockage, and its relationship to propeller performance for small scale UAV applications. First, the experimental set-up used to characterise the blockage effect is described. Results of wind tunnel tests are then presented and discussed, and a comparison is made with blockage effects for larger general aviation propellers.

Experimental Set-up

The 7 by 5 ft (2.13 m by 1.52 m) low speed wind tunnel of The University of Sydney is used to test propellers over a range of rotational and wind tunnel speeds. The closed-loop tunnel can operate over a speed range from 2 to 42 m/s.

Two series of tests are conducted for the propeller tests. In the first series of tests the ‘un-installed’ performance of the propeller is measured. For these tests, the propeller is operated without a fuselage as shown in Figure 1. The propeller is driven by a Scorpion SII-3032-990 kV brushless outrunner motor which is controlled via a Castle Creations ICE-75 electronic speed controller (ESC). The ESC is programmed in governor mode so that the rotational speed of the propeller is

held constant throughout the run, regardless of the wind tunnel speed. Power is provided by an ET-system LAB/SMS 435 power sources. Forces and moments are measured using an ATI Mini45 6 component load cell. Load cell measurements are taken at a frequency of 1000 Hz and the average value over a 2 second test period is logged.

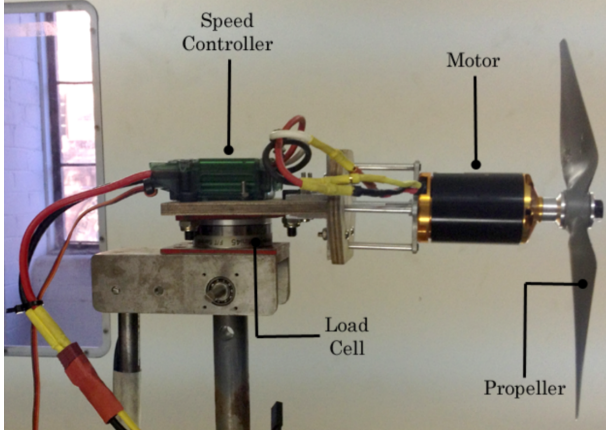


Figure 1: Set-up to measure un-installed propeller performance.

For the second series of tests, where the “installed” performance is measured, the same set-up is used but a fuselage is added. The propeller is installed in a puller configuration and a teardrop shape fuselage is used [19], as shown in Figure 2. The teardrop puller fuselage is CNC-ed from an acetal thermoplastic and has a maximum diameter of 13 cm.

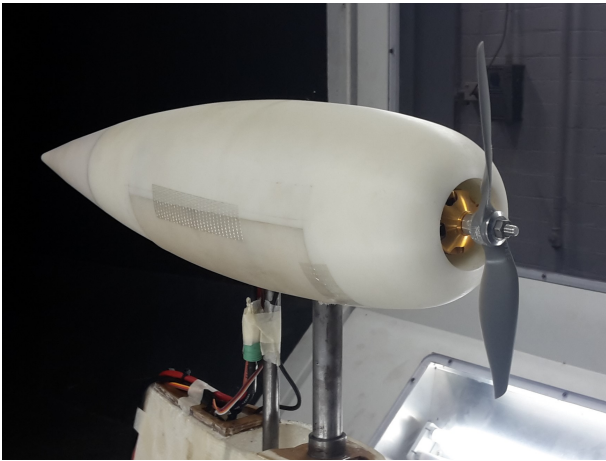


Figure 2: Puller installation.

Inaccuracies arise in the measurement of the freestream velocity as a result of the change in static pressure caused by the propeller slipstream. This increase in pressure leads to a velocity measurement larger than the true freestream velocity. This is corrected as follows [20]:

$$\frac{V'}{V} = 1 - \frac{\tau_4 \cdot \alpha_1}{2 \cdot \sqrt{1 + 2 \cdot \tau_4}} \quad (2)$$

with:

$$\tau_4 = \frac{T}{\rho \cdot A \cdot V^2} \quad \alpha_1 = \frac{A}{C} \quad (3)$$

A is the propeller disk area, C is the cross-section area of the test section, T is the propeller thrust, V the freestream velocity, and ρ the air density.

The second correction addresses the local velocity increase caused by the blockage of the wind tunnel mount and test object. This increase in velocity is related to the relative volume of the test piece and overall test section. The relative increase in velocity is given by [20]:

$$\frac{V'}{V} = \frac{K \cdot \tau \cdot \mathcal{V}}{A^{3/2}} \quad (4)$$

where $K = 1.045$, $\tau = 0.92$ and \mathcal{V} is the volume of the fairing and fuselage (where applicable).

For tests with a fuselage installed, a third correction is applied to correct for the slowing down of the air at the propeller disk due to the presence of the fuselage. The propeller advance ratio J is therefore corrected as follows [21]:

$$J_{eff} = J \cdot (1 - h) \quad (5)$$

where:

$$h = 0.329 \frac{S_c}{D^2} \quad (6)$$

where J_{eff} is the effective advance ratio and S_c is the fuselage area in the propeller slipstream. The advance ratio is defined as:

$$J = \frac{V}{n \cdot D} \quad (7)$$

where n is the rotational speed of the propeller.

Results

Results of the wind tunnel tests are given for 3 different propellers. All propellers are manufactured by APC propellers [22], and are of the thin electric series. The propellers tested are the APC 8x8, 9x9, and 10x10 where the first number indicates the propeller diameter (in inches) and the second number indicates the propeller pitch (in inches). These specific propellers were selected as they all have a ratio of pitch to diameter of unity. Whereas this is a relatively high pitch ratio, this allows isolation of the effect of the blockage ratio without any effect of relative pitch variations.

For each of the tests, the measured thrust coefficient C_T , power coefficient C_P , and efficiency η are reported in function of the advance ratio J :

$$C_T = \frac{T}{\rho \cdot n^2 \cdot D^4} \quad (8)$$

$$C_P = \frac{P}{\rho \cdot n^3 \cdot D^5} \quad (9)$$

$$\eta = \frac{T \cdot V}{P} \quad (10)$$

where T is the propeller thrust, and P the propeller power.

First results of the tests without fuselage are given. After that a comparison is made with the tests with the fuselage present.

Un-installed Performance

The thrust coefficient, power coefficient, and efficiency for the uninstalled propeller tests are given in Figures 3, 4, and 5. Results for one rotational speed are given for each propeller, and a speed in the middle of the operational range is selected so that a similar motor power is required for each test. As shown in Figures 3 and 4, the measured thrust and power coefficient are moderately affected by the propeller diameter. Both slightly

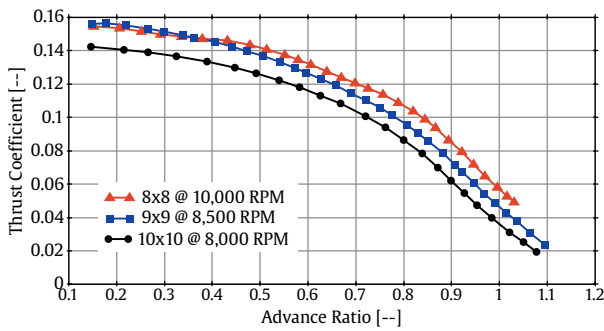


Figure 3: Uninstalled thrust coefficient as function of advance ratio.

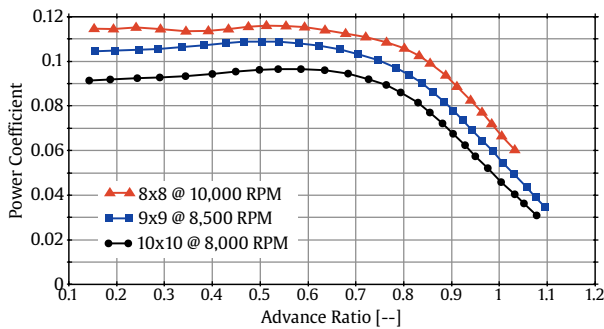


Figure 4: Uninstalled power coefficient as function of advance ratio.

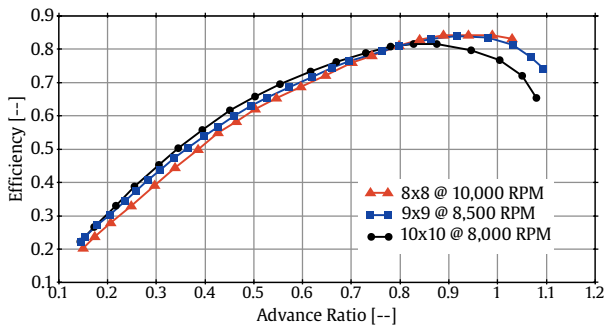


Figure 5: Uninstalled propeller efficiency as function of advance ratio.

reduce with an increase in propeller diameter despite the operating Reynolds numbers being kept constant due to the change in the rotational speed for each propeller.

As shown in Figure 5, the peak efficiency of all 3 propellers is close to 85%. Whereas fairly high this is consistent with similar tests reported by other researchers [7, 8]. The peak efficiency occurs at an advance ratio close to 1 for both the 8x8 and 9x9 propeller. The 10x10 propeller has a peak efficiency that occurs at a slightly lower advance ratio, which could be due to a slight difference between the real advance ratio and that specified by the manufacturer [23].

Installed Performance

Results from the tests with the propeller installed in front of the teardrop fuselage are reported in Figures 6, 7, and 8. Results of tests with the fuselage are indicated with dashed lines on those figures. Uninstalled results are included as solid lines to allow an easy comparison. As can be seen from Figure 6 the reduc-

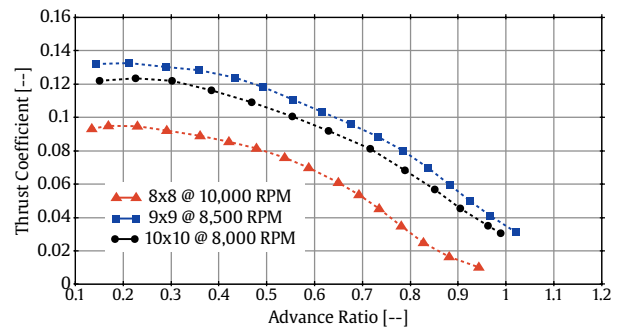


Figure 6: Installed thrust coefficient as function of advance ratio.

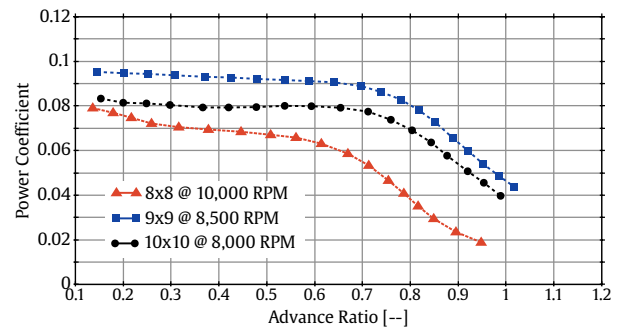


Figure 7: Installed power coefficient as function of advance ratio.

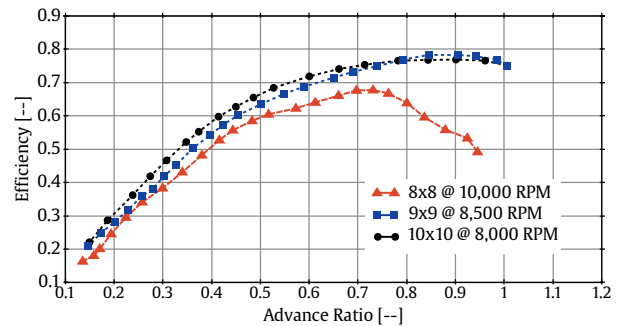


Figure 8: Installed propeller efficiency as function of advance ratio.

tion in thrust depends strongly on the blockage ratio. Whereas a thrust reduction of around 15% is found for the 10x10 propeller, the reduction for the 8x8 propeller is close to 50%. A similar trend is observed for the power coefficient, albeit with slightly smaller reductions. The power required to turn the 10x10 propeller is reduced by around 12%, while the 8x8 propeller requires around 40% less power at a given advance ratio.

The combined effect of the reduction in thrust and power coefficient is reflected in the change in propeller efficiency. As shown in Figure 8 a drop in peak efficiency of close to 10% is obtained for both the 9x9 and 10x10 propellers. The effect for the 8x8 propeller is much more pronounced with a drop in peak efficiency of over 15%. The advance ratio at which the peak efficiency occurs is also much more affected for the 8x8 propeller.

Table 1 summarizes the drop in peak efficiency for the different propellers and compares it with predictions from correlations derived from measurements for general aviation propellers [18].

The drop in peak efficiency for the two larger propellers is in line with the predictions. However, the drop in peak efficiency for the smaller propellers is much more pronounced. This suggests that the critical blockage ratio for small propellers could be higher than that for larger propellers. This could partially stem from the increase in boundary layer thickness as the tests reported here are conducted at much lower Reynolds number conditions than those from which the correlations presented in ref. [18] are derived.

	B	Measured $\Delta\eta_{max}$	Predicted $\Delta\eta_{max}$
8x8	0.64	19.3%	11.0%
9x9	0.57	6.6%	7.6%
10x10	0.51	6.0%	5.2%

Table 1: Comparison between measured and predicted efficiency change

Conclusions

When operating in the proximity of a fuselage, the performance of a propeller can be significantly affected by the fuselage blockage. Whereas well characterized for larger general aviation propellers, these effects remain largely uncharted for small propellers used on unmanned aircraft. The current article presents results of wind tunnel tests of three small propellers with and without a fuselage. It is shown that the blockage effect can be more pronounced for small propellers than for larger propellers and can lead to a reduction in efficiency of close to 20%. A commensurate reduction in endurance can be expected.

Acknowledgements

The authors would like to thank Pierre-Yves Monjo for his assistance in the experimental campaign as part of an internship at The University of Sydney.

References

- [1] <https://www.whitehouse.gov/the-press-office/2016/06/21/fact-sheet-enabling-new-generation-aviation-technology>, Last Accessed: August, 2016.
- [2] Logan, M.J., Chu, J., Motter, M.A., Carter, D.L., Ol, M., and Zeune, C., *Small UAV Research Evolution in Long Endurance Electric Powered Vehicles*. AIAA Infotech Aerospace 2007 Conference and Exhibit, Nohnert Park, CA, AIAA-2007-2730.
- [3] Verstraete, D., Gong, A., Lu, D. D.-C., and Palmer, J.L., Experimental investigation of the role of the battery in the AeroStack hybrid, fuel-cell-based propulsion system for small unmanned aircraft systems. *International Journal of Hydrogen Energy*, 40(3): 15981606, 2015.
- [4] Gong, A., Palmer, J.L., Brian, G., Harvey, J.R., and Verstraete, D., Performance of a hybrid, fuel-cell-based power system during simulated small unmanned aircraft missions. *International Journal of Hydrogen Energy*, 41(26):1141811426, 2016.
- [5] Gong, A., and Verstraete, D., *Role of battery in a hybrid electrical fuel cell UAV propulsion system*, 52nd Aerospace Sciences Meeting AIAA SciTech, National Harbor, MD, AIAA 2014-0017.
- [6] Gur, O., and Rosen, A., Optimizing electric propulsion systems for unmanned aerial vehicles, *Journal of Aircraft* 46(4),1340-1353,2009.
- [7] Nelson, J.T., *Practical Modifications for Low Reynolds Number Propeller Applications*. Master's thesis, Wichita State University, December 2009.
- [8] Merchant, M.P., *Propeller Performance Measurement for Low Reynolds Number Unmanned Aerial Vehicle Applications*. Master's thesis, Wichita State University, December 2005.
- [9] Ol, M., Zeune, C., and Logan, M., *Analytical/Experimental Comparison for Small Electric Unmanned Air Vehicle Propellers*. 26th AIAA Applied Aerodynamics Conference, Honolulu, HA, AIAA-2008-7345.
- [10] Brandt, J.B., and Selig, M.S., *Propeller Performance Data at Low Reynolds Numbers*. 49th AIAA Aerospace Sciences Meeting, Orlando, FL, AIAA-2011-1255.
- [11] Wald, Q.R., *The Aerodynamics of Propellers*, *Progress in Aerospace Sciences*, 42(2):85-128, 2006.
- [12] Jones, B., *Elements of Practical Aerodynamics*, John Wiley & Sons, Inc., 3rd ed., 1942.
- [13] Lan, C.E., and Roskam, J., *Airplane Aerodynamics and Performance*. Roskam Aviation and Engineering, 1997.
- [14] McHugh, J.G., and Derring, E.H., *The Effect of Nacelle-Propeller Diameter Ratio on Body Interference and on Propeller and Cooling Characteristics*, National Advisory Committee for Aeronautics, NACA-TP-680, 1939.
- [15] Bailey Oswald, W., *General Formulas and Charts for the Calculation of Airplane Performance*, National Advisory Committee for Aeronautics, NACA-TP-408, 1932.
- [16] Weick, F.E., *Full Scale Wind Tunnel Tests with a Series of Propellers of Different Diameters on a Single Fuselage*, National Advisory Committee for Aeronautics, NACA-TP-339, 1931.
- [17] Weick, F.E., *The Effect of reduction Gearing on Propeller-Body Interference as shown by Full Scale Wind Tunnel Tests*, National Advisory Committee for Aeronautics, NACA-TP-338, 1931.
- [18] Lowry, J.T., *Performance of Light Aircraft*, AIAA Library of Flight, AIAA, Reston, VA, 1999.
- [19] Lennon, A., *Basics of R/C Model Aircraft Design: Practical Techniques for Building Better Models*, AIAA Library of Flight, Air Age, 1996.
- [20] Pope, A., Barlow, J.B., and Rae, W.H., *Low Speed Wind Tunnel Testing*, John Wiley & Sons, 3rd ed., 1999.
- [21] Torenbeek, E., *Synthesis of subsonic aircraft design*, Delft University Press, 1976.
- [22] <https://www.apcprop.com>, Last Accessed: August, 2016.
- [23] McCrink, M.H., and Gregory, J.W., *Blade Element Momentum Modeling of Low-Re Small UAS Electric Propulsion Systems*, 33rd AIAA Applied Aerodynamics Conference, Dallas, TX, AIAA-2015-3296.